ANALYSIS OF IMPACT RESPONSE AND DAMAGE IN COMPOSITE LAMINATES AND COMPONENTS

[1]Vinay M Bashettiyavar, [2]Manjunath S B

[1]Post Graduation Student, [2]Assistant Professor
[1]Department of Mechanical Engineering,
[1]Dayananda Sagar College of Engineering, Bengaluru, India.

Abstract: The composite is a combination of two or more materials that are combined at a macroscopic level and are not soluble in each other. Fibre-reinforced composites are popularly known for their supreme properties such as high strength to weight ratio, high impact strength, high fatigue resistance, etc. Hence they are most commonly used in Aerospace, Automotive, Marine structures, and Defence sectors. Composites have high strength in the direction of the fibre, lesser in strength in the transverse direction. Transverse loads cause Barely Visible Impact Damage (BVID) which results in catastrophic failure of composites and structure. BVID has been the topic of continual research due to its complexity in early detection and prevention. In present study Low-velocity impact response and damage analysis of CFRP and stiffened CFRP laminates using finite element modeling with LS-DYNA has been performed for assessing delamination at the interface and influence of other parameters such as material models, the influence of stiffener and influence of impactor shape on the impact response the composite material is also studied.

Index Terms - **Composite, Impact response, Impact damage, barely visible impact damage.**

I. INTRODUCTION

Composite materials, have been used from past few decades which plays an important role in day today day life because of their supreme properties such as high strength, high stiffness, light in weight, high impact resistance, low thermal conductivity, corrosion free and radar transparent, which made the conventional materials are replaced by composites. Because of these versatile properties, composite materials have been widely used in various engineering sectors such as aerospace, automotive, biomedical industries, civil engineering, defence industries, shipping industries, sports industries, etc.

Composite materials are formed by the combination of two or more materials that are combined at a macroscopic or microscopic level which are not soluble in each other and retain their characteristics when combined to achieve required properties. Composites have very high strength in the direction of the fibre, lesser in strength in the transverse direction. The impact behaviour of composite laminate has been treated extensively in the technical literature. A comprehensive literature overview on the impact on composite structures is given by Abrate [1]. As discussed above composites have great advantages over conventional materials, in spite of having these advantages, these materials are also susceptible to damages under transverse impact loads and the nature of damage induced in the composite due to such impacts are completely different than that in the case of conventional materials [2]. These transverse loads cause Barely Visible Impact Damage (BVID) which results in catastrophic failure of composites and structure, some of the examples which cause BVID is by dropping tool during maintenance and flying debris on the runway striking the aircraft during takeoff or landing. BVID has been the topic of continual research due to its complexity in early detection and prevention [3]. These impact loads are classified on the bases of body, velocity, energy interaction, etc. Some of them are a hard body impact, soft body impact, vehicle crash, low-velocity impact, high-velocity impact, and hypervelocity impact. The velocity up to 8 m/s and energy interaction up to 50 joules are classified as low velocity impact, velocities up to 70 m/s and energy interaction up to 50 joules are classified as intermediate velocity impact, impact velocity up to 300-2500 m/s and energy interaction up to 10kJ- 20kJ is considered as high velocity impact and the impact speed above 3000 m/s is classified as hypervelocity impact. The classification of low velocity impact is based on the existence of damage occurred. Delamination and matrix crack is due to low velocity impact, whereas fibre break and penetration are due to high velocity impact. The damage is more severe during the small mass impact when compared to large mass drop weight [4].

Composite Panels stiffened with attached stiffeners are frequently used in aerospace, naval, long span bridge decks, ship deck hulls and various civil engineering structures when structural weight is an important concern. Laminated composite stiffened panels are anisotropic and orthotropic in nature. Laminated composite stiffened panels are most commonly used structural elements in weight sensitive structure applications, which are made by adjoining of laminated composite plate and stiffeners. Laminated composite plates are made by stacking of lamina with different orientation of the principle material direction. The stiffened panel consists of the laminated composite plate provided with stiffeners in the longitudinal and/or transverse direction. There are different types of the stiffener, they are classified as the open type and closed type or box type. Open type stiffeners are torsionally week in stiffness as compared closed type or box type. Figure 1 shows a schematic representation of the different type of stiffeners. Some various shaped stiffening members commonly used for panel structural concepts are “T”, “Z”, “I”, “C”, “J”, and hat [5]. In this present study, hat stiffeners are used. The objectives of this article are to study Low-velocity impact response and damage analysis of simple CFRP laminate with the delamination interface contact and stiffened CFRP laminate using finite element modelling with LS-DYNA and validating the results of simple CFRP plate with the benchmark problem taken from the paper Simulation of Low velocity impact on composite plate with compressive preload [6]. The effect of impactor shape on the low velocity impact response is also studied.

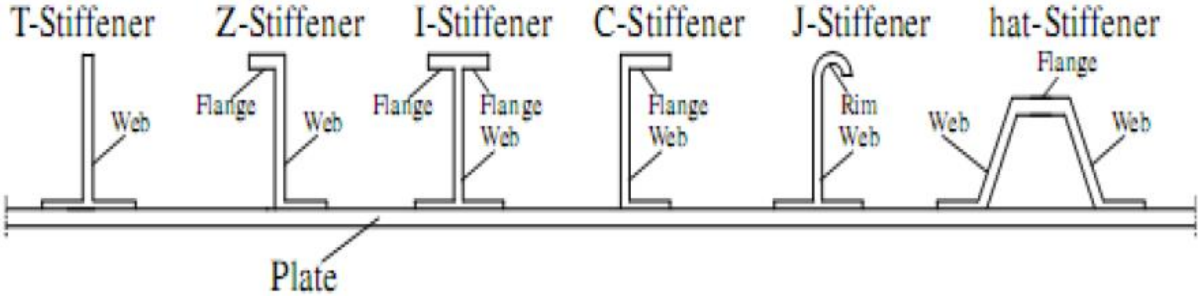

Figure 1 Examples for Stiffener cross section [5].

II. Benchmark Validation

This chapter emphasizes the development of the finite element model for impact analysis of composite structures using the finite element analysis package LS-DYNA. A benchmark problem is considered for validation of the finite element model. The problem of the low-velocity impact of a spherical impactor on a composite plate for which the experimental results are available in the literature[8].

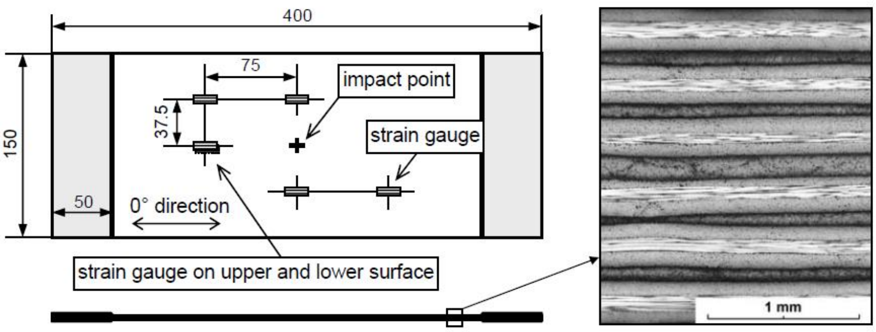

Figure 2 Experimental impact test specimen (All dimensions are in mm) and micrograph of composite laminate [6].

The problem involves the low velocity impact on a carbon fibre reinforced laminated composite plate having the stacking sequence of [-45°/0°/45°/90°] $_{3s}$. The dimensions of the laminate are 400 x 150 x 2.7 mm, the lateral ends on either side were clamped (50mm each side); the final length of the laminate reduces to 300 x 150 x 2.7 mm. A total of six strain gauges were applied on the laminate, five on the upper surface and one on the lower surface. These strain gauges give valuable information such as force, energy absorption and displacements. The laminate is impacted by a spherical steel impactor of diameter 25.4mm and the mass of the impactor is 1.85kg. To limit the complexity of the study the energy level of 40 Joule was kept constant. Since the impactor mass was constant, this corresponds to an impactor velocity of 6.5 m/s. The experimental test specimen with its micrograph and the experimental test rig is shown in Figure 2 and Figure 3 respectively.

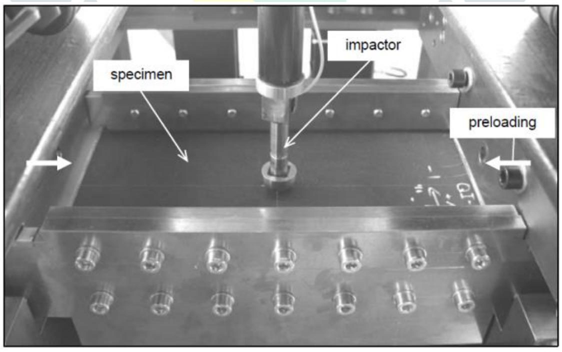

Figure 3 Experimental Impact test rig [6].

2.1 Finite Element Model Development

The FE model for the low velocity impact simulation is developed in commercial Finite Element package tool LS-DYNA which involves the modelling of the composite material including intra-laminar failures. The composite plate contains 24 plies of unidirectional carbon fibre epoxy polymer of the orientation [-45°/0°/45°/90]$_{3S}$. Since the plate length and width dimensions are large compared to the thickness, a 2D modelling approach with shell elements is adopted. The laminate was modeled using Belytschko-Lin-Tsay (ELFORM 2) shell element which has 6 degrees of freedom at each node. The continuum shell elements have the capability of simulating systems that are globally three dimensional but locally planer [7]. There are the different composite material model for shell element in LS-DYNA, the linear elastic model MAT54 MAT_ENHANCED_COMPOSITE_DAMAGE was used, which deals with the Chang/Chang failure criteria. In Chang/Chang criteria the damage occurs as soon as one of the four criteria is met, which are shown below.

Tensile failure in fibre direction:
$$e_{f,t}^2 = \left(\frac{\sigma_1}{XT}\right)^2 + \beta\left(\frac{\tau_{12}}{SC}\right)^2 - 1\begin{cases}\geq 0\ failure\\ < 0\ elastic\end{cases} \quad (1)$$

Compressive failure in fibre direction:
$$e_{f,c}^2 = \left(\frac{\sigma_1}{XC}\right)^2 - 1\begin{cases}\geq 0\ failure\\ < 0\ elastic\end{cases} \quad (2)$$

Tensile failure in matrix direction: $$e_{m,t}^2 = \left(\frac{\sigma_2}{YT}\right)^2 + \left(\frac{\tau_{12}}{SC}\right)^2 - 1 \begin{cases} \geq 0 \ failure \\ < 0 \ elastic \end{cases} \quad (3)$$

Compressive failure in matrix direction: $$e_{m,c}^2 = \left(\frac{\sigma_2}{2SC}\right)^2 + \frac{\sigma_2}{YC}\left(\frac{YC^2}{4SC^2} - 1\right) + \left(\frac{\tau_{12}}{SC}\right)^2 - 1 \begin{cases} \geq 0 \ failure \\ < 0 \ elastic \end{cases} \quad (4)$$

The material properties used for modelling the composite material in this study is shown in Table 1

Table 1 Elastic and Failure properties of CFRP laminate [6].

Parameters	Material	ρ [g/cm³]	E_{11} [GPa]	E_{22} [GPa]	E_{12} [GPa]	υ_{12} [-]	XT [MPa]	XC [MPa]	YT [MPa]	YC [MPa]	SC [MPa]	DFAILT	DFAIL C	DFAIL M	DFAIL S
Defined Value	CF/EP laminate	1.6	153	10.3	5.2	0.3	2540	1500	82	236	90	0.017	-0.0135	0.1	0.03

The impactor was modeled as a spherical rigid body using the 8 noded solid elements (ELFORM 1) which has three degrees of freedom for each node and the MAT20 MAT_RIGID material model was used. The initial velocity of 6.5 m/s is defined in the negative z-direction by using INITIAL_VELOCITY card. The clamping conditions of the CFRP laminate include fixed support of the longitudinal edges and simple support of the lateral edges. A segment based CONTACT_AUTOMATIC_SURFASCE_TO_SURFACE was established between the impactor and the composite plate with SOFT=2. The impact event will last approx to 7 ms. The FE model is shown in Figure 4.

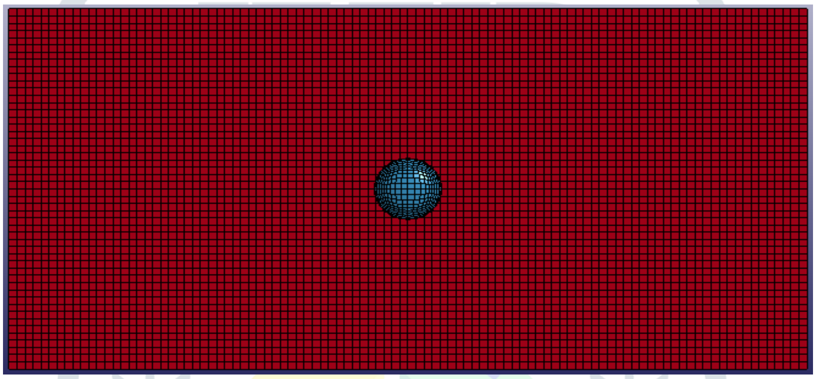

Figure 4 Finite Element Model of laminate and impactor.

2.2 Comparison between Simulation results and Experimental Results

In this section, the simulation results are presented and compared with the experimental results. The following data such as Impact contact force, Energy and the displacement data were evaluated.

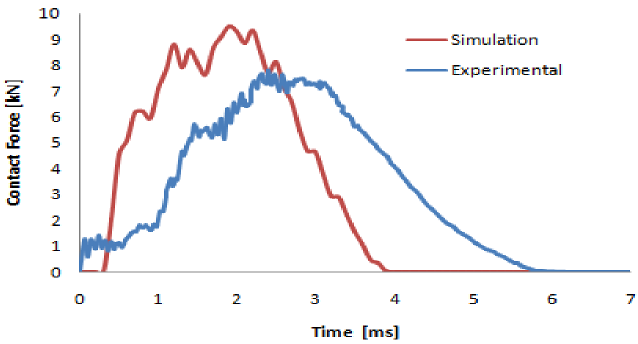

Figure 5 Contact force plot of experimental and simulation results

2.2.1 Impact contact force

The intensity of the impact contact force variation with the time is generated. Figure 5 shows the correlation of the Impact contact force v/s time history between the experimental and the simulation results. The maximum impact contact force in the FE simulation is 9.5kN ware as in the experimental result it was 8kN. There is some deviation in the FE results as compared to experimental values, because of on availability of the actual time step size used in an experimental test conducted.

2.2.2 Contact energy

The inverted kinetic energy was plotted in both experimental and simulation conditions. Figure 6 shows the Energy v/s Time plot. The maximum energy attained in finite element simulation was 38 J and the experimental was 40 J. The energy absorption values during the impact are in close correlation and the energy absorbed during the simulation was 14.4 J whereas in experimental it was 13.2 J.

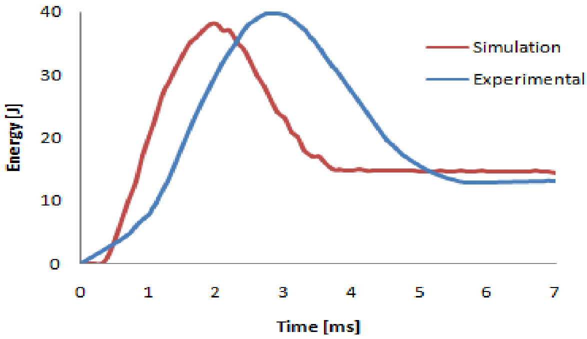

Figure 6 Energy plot for experimental and simulation results

2.2.3 Displacement plots

The displacement v/s time history of the laminate is shown in Figure 7. The maximum displacement was found to be 9.96 mm comparing to the experimental there is no much difference in the displacement of the laminate

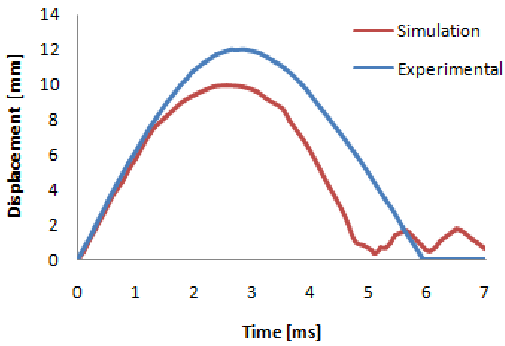

Figure 7 Displacement plot for experimental and simulation results

2.2.4 Intralaminar damages for Benchmark Problems

The intralaminar damage for the benchmark problems was studied. Figure 8 shows the failure contour of top and bottom lamina during maximum impact duration (time 1.9 ms). The region gets failed as the failure criterion reaches the value 1.

Failure of Fiber in Tension mode

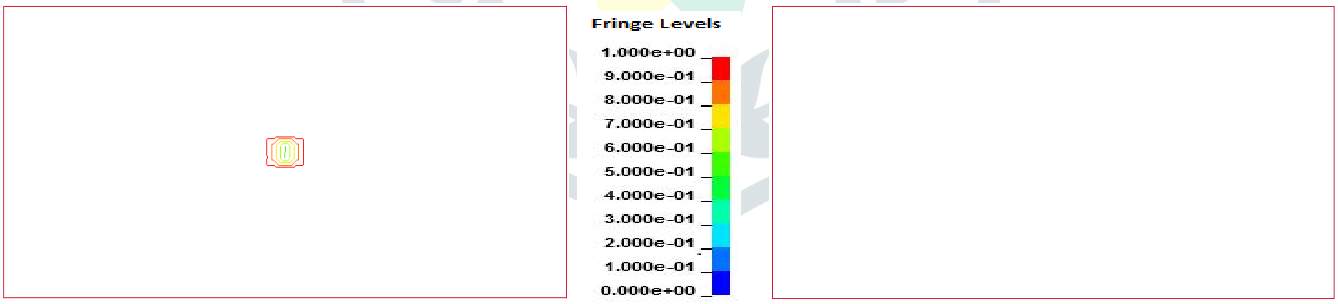

Top Layer at 1.9 ms **Bottom Layer at 1.9 ms**

Failure of Fiber in Compression mode

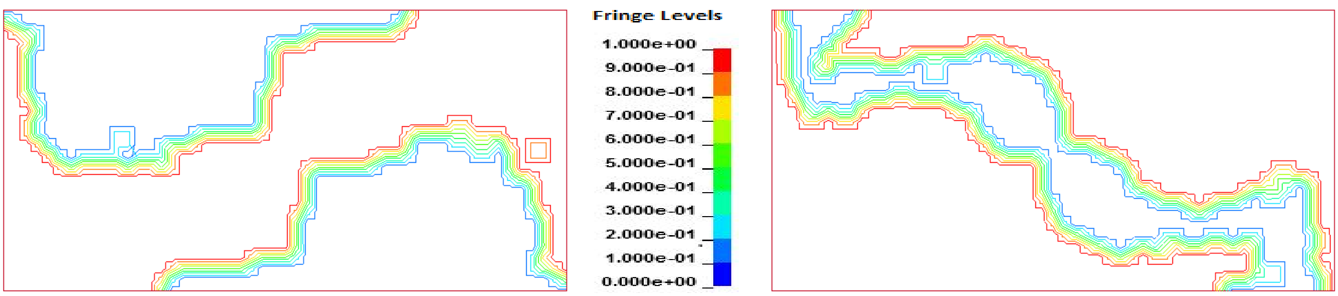

Top Layer at 1.9 ms **Bottom Layer at 1.9 ms**

Failure of Matrix in Tension mode

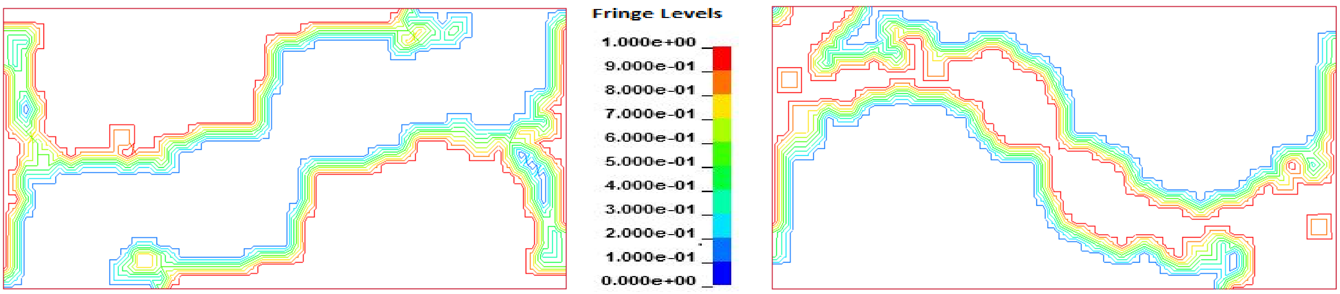

Top Layer at 1.9 ms **Bottom Layer at 1.9 ms**

Failure of Matrix in Compression mode

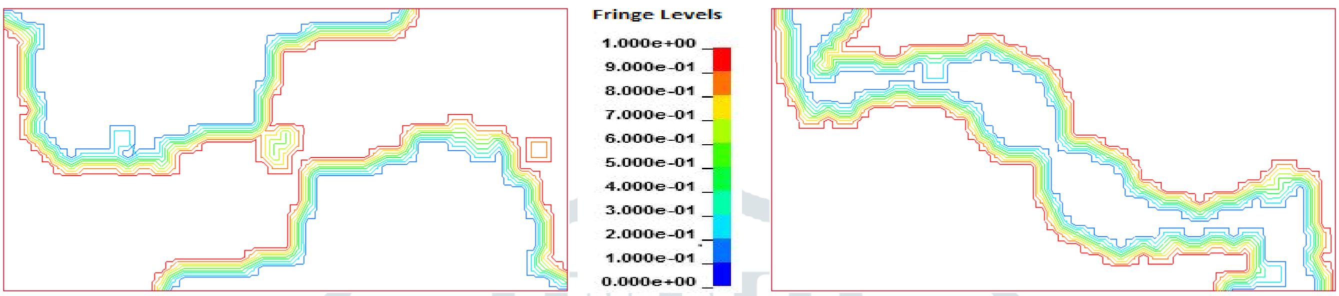

Top Layer at 1.9 ms **Bottom Layer at 1.9 ms**

Figure 8 Fibre and matrix failure contour for the Benchmark problem

III. DELAMINATION

Delamination is the major issue in the composite laminates. Composite laminate involves the presence of both the interlaminar and intralaminar damage mechanisms. The fibre fracture and matrix cracking are called as intralaminar damages whereas interlaminar damages include delamination and later penetration. Delamination means separation of the adjacent laminas, which is occurred due to the mismatch of the bending stiffness between the adjacent laminas.

There are various methods to access the onset of delamination. Some of them are Fracture mechanics approach, continuous damage modeling, cohesive zone modelling and others. In the present study, continuous damage modeling technique is adopted. There are different methods for modelling Delamination, such as cohesive zone modeling, Tie-Break contacts. In the present study, tiebreak contacts are used as adhesive to bond the sublaminates in the LS-DYNA models. Tiebreak contacts are active for nodes which are initially in contact. Normal and shear failure strength must be defined for tiebreak contact to check the bond failure. Tiebreak contact acts the same way as other common contacts under compressive load. During the loading, the damage of the material is a linear function of the distance between the two points which are initially in contact. When the critical opening is reached, the contact will be broken and the sublaminates are converted into two separate surfaces with the regular surface to surface contact between them to prevent penetrations. Under tensile load, tiebreak allows the separation of the surfaces and ultimately the failure of the tied surfaces will occur under the following failure criterion:

$$\left(\frac{|\sigma_n|}{NFLS}\right)^2 + \left(\frac{|\sigma_s|}{SFLS}\right)^2 \leq 1 \qquad (5)$$

Where NFLS is tensile failure strength and SFLS is shear failure strength of the adhesive.

An adhesive material with the properties of NFLS = 56 MPa and SFLS = 44 MPa has been chosen. These are typical properties for epoxy adhesives usually used in structural applications. Different contact definitions are needed between components in the model. CONTACT_AUTOMATIC_SURFACE_TO_SURFACE are used between impactor and plates and CONTACT_AUTOMATIC_ONE_WAY_SURFACE_TO_SURFACE_TIEBREAK is used between sublaminates of the composite plate in the model. OPTION 8 in contact card was used for simulation of crack propagation based on the cohesive zone model, implemented in LS-DYNA as a delamination contact [8].

3.1 Finite element modeling

The finite element modeling of the sublaminates is shown in Figure 9. The two sublaminates are modeled using Belytschko-Lin-Tsay shell element and the impactor was modeled using solid element. The boundary conditions and the impactor velocity remains the same as in single shell modeling.

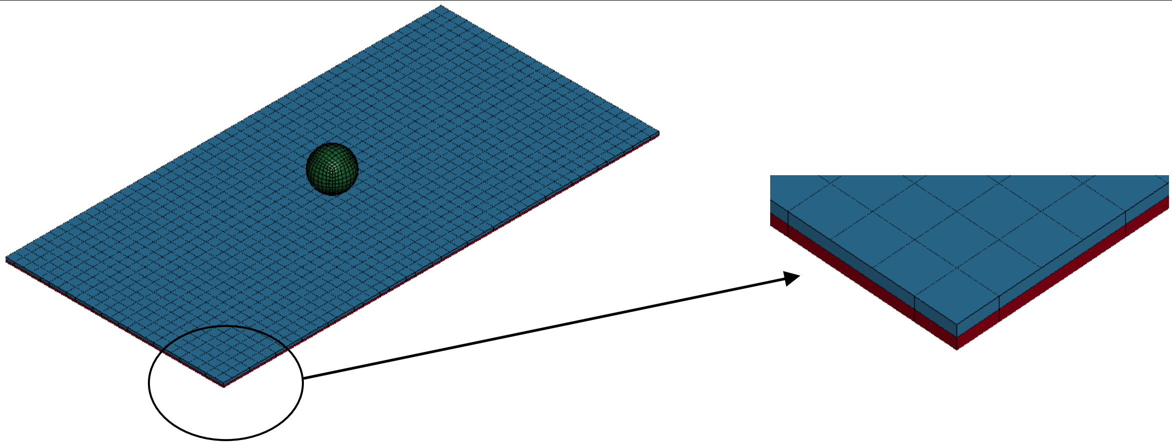

Figure 9 Finite Element modeling of sublaminates

3.2 Results and Discussions

3.2.1 Energy plot

The impact damage and impact response for the problem was studied to benchmark problem. The energy plot is shown in Figure 10. The increase in energy absorption was seen as compared to the single shell model. In the single shell model or the model without delamination contact, the lowest value of the absorbed energy is seen. This is because there is no interlaminar damages can occur in the model. This means, the more the delamination contact interfaces are used, the more the reduction of the bending stiffness of the plate. Due to the reduction in the bending stiffness the energy absorption increases. The energy absorption was found to be 18.2 J.

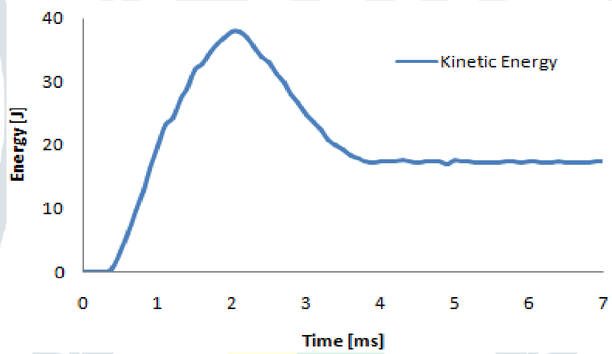

Figure 10 Energy Plot for Sublaminates

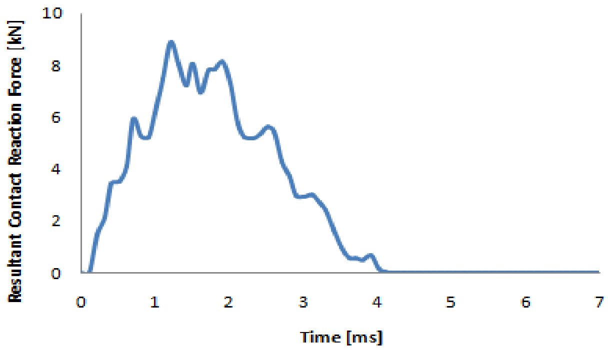

Figure 11 Contact force history of Sublaminates

3.2.2 Impact contact force history

The contact force history is shown in Figure 11, it is seen that there is a decrease in the contact force between the components due to delamination triggered by the element deletion when it reaches the failure criteria. The maximum impact force was in the two shell model was found to be 8.88kN.

3.2.3 Displacement Plot

The deflection or the displacement of the model having delamination contact interface in between the shells (i.e. two shell model) was found to be higher than the model without delamination contact. This is because of the reduction in the stiffness. The displacement was found to be 10.84 mm as shown in Figure 12.

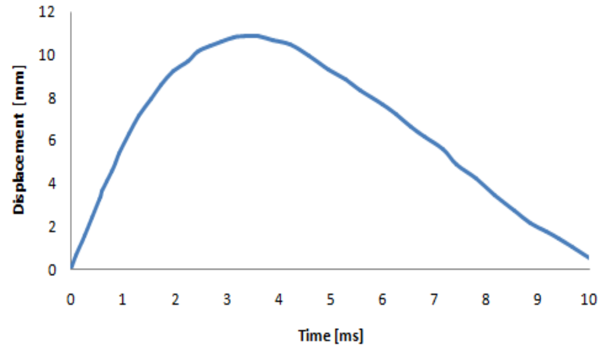

Figure 12 Displacement v/s Time history of Sublaminates

3.2.4 Interlaminar Damage

Interlaminar damages include delamination and later penetration. Delamination is caused due to the separation of the adjacent laminas, which is occurred due to the mismatch of the bending stiffness between the adjacent laminas. Onset delamination can be detected using Delamination Threshold Load. It is the load at which the delamination onset takes place. The sudden drop in the contact force history is the sign of delamination caused by the reduction of the stiffness in the sublaminates. Delamination onset occurs when the delamination threshold load drops below the maximum impact load [9] G. A. Schoeppner et al. experimentally demonstrated the delamination onset based on contact force history. Figure 13 shows the Delamination threshold load value.

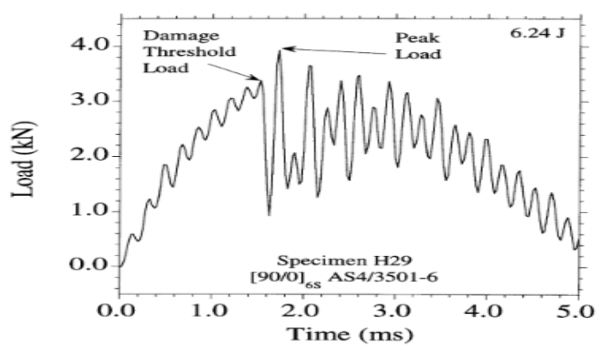

Figure 13 Delamination threshold load determination [9].

Hence from Figure 10, it is seen that there is a drop in the contact force history before the maximum peak force is attained. The maximum impact force was found to be 8.88kN and the delamination threshold load at which the onset delamination takes place was found to be 5.89kN. The contact force history and the magnified image of the peak load attained and the delamination threshold load is shown in Figure 14.

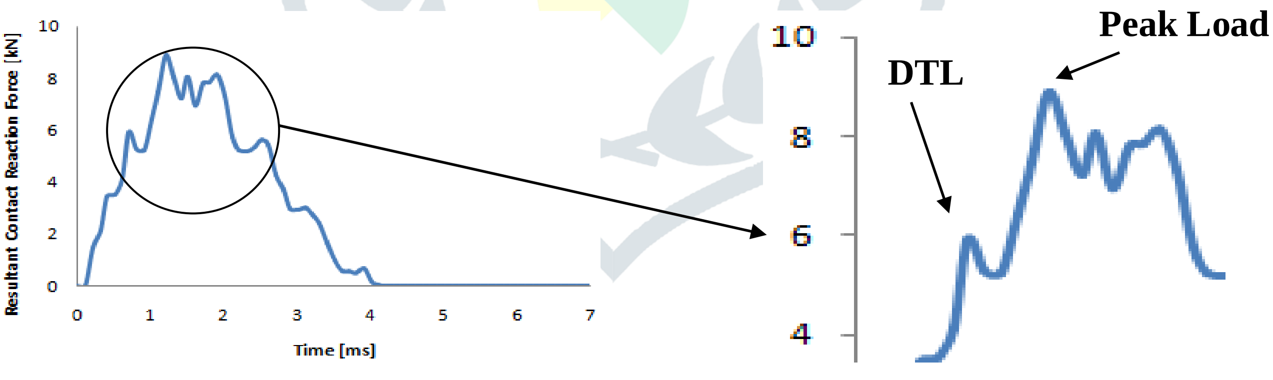

Figure 14 Delamination threshold load for Sublaminates

3.2.5 Intralaminar Damages

Fibre fracture and matrix cracking under tension and compression mode are some of the intralaminar damages which are commonly seen in the composite laminates. The intralaminar damages of all 24 lamina for the two shell model are shown in Figure 15. Red indicates the failure region and blue indicates less damage zone.

Failure of Fiber in Tension mode

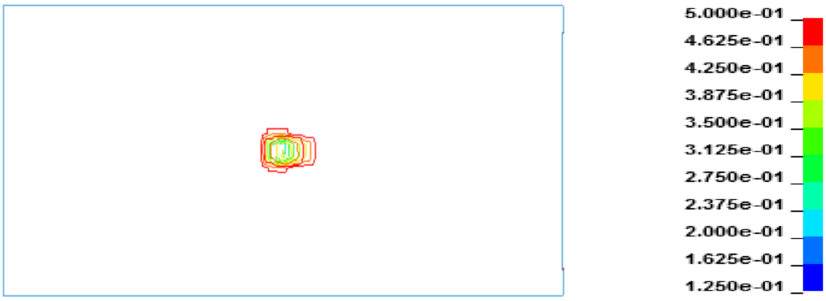

Failure of Fiber in Compression mode

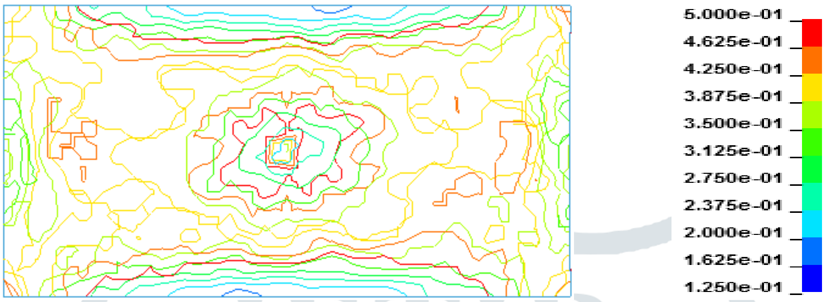

Failure of Matrix in Tension mode

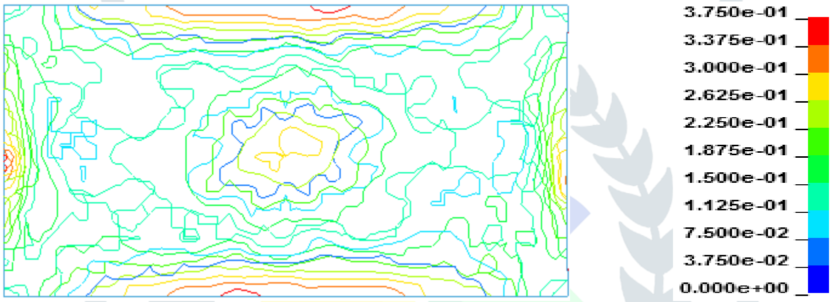

Failure of Matrix in Compression mode

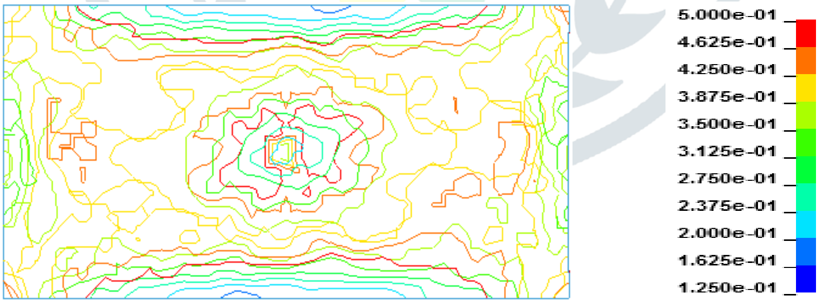

Figure 15 Intralaminar failures two shell model

IV. INFLUENCE OF MATERIAL MODEL

Material models have a great influence on the response and damage of a composite laminate. In the present study, the influence of the material models such as MAT 54 and MAT 55 was studied. The failure responses and the damages for single-shell and two-shell models studied above were based on MAT 54 (i.e. using Chang-Chang Failure criteria). Here will study the influence of material mode MAT 55 on the composite laminates.

Material model MAT 55 was suggested by Tsai-Wu which is called as Tsai-Wu matrix failure criteria. Material model MAT 55 formulation is very close to material model MAT 54. It uses Tsai-Wu failure criteria for compressive and tensile matrix failure modes which are given in the single expression as follows.

$$\frac{\sigma_{22}^2}{Y_C Y_T} + \left(\frac{\sigma_{12}}{X_S}\right)^2 + \frac{(Y_C - Y_T)\sigma_{22}}{Y_C Y_T} = 1 \quad (6)$$

This material model is same as Chang-Chang failure model except the compressive and tensile matrix failure mode is replaced by the above expression. Transverse shear is not considered in this model [10]. The comparative results of impact response and impact damages for MAT 54 and MAT 55 are shown below

4.1 Results and Discussion

4.1.1 Energy Plot

The energy plots of the material model MAT 54 and MAT 55 is shown in Figure 16. From the plot, it is seen that the energy absorption of a shell modeled using MAT 55 is slightly higher as compare to MAT 54. The energy absorption in shell modeled using MAT 55 was found to be 16.27 J whereas in the shell modeled using MAT 54 is 14.4 J.

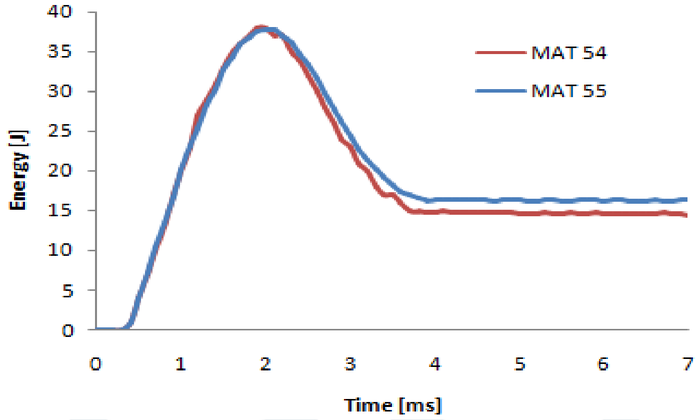

Figure 16 Energy plots for Material model MAT 54 and MAT 55

4.1.2 Intralaminar Damages

Intralaminar damages for the single shell model, modeled using the material model MAT 55. The failure contour of the top and bottom lamina during the maximum impact force duration (time- 2.1 ms) is shown in Figure 17.

Failure of Fiber in Tension mode

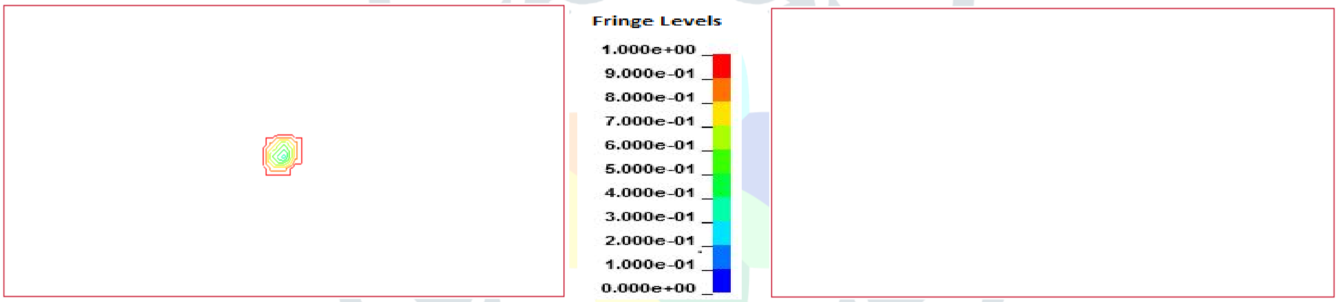

Top Layer at 2.1 ms **Bottom Layer at 2.1 ms**

Failure of Fiber in Compression mode

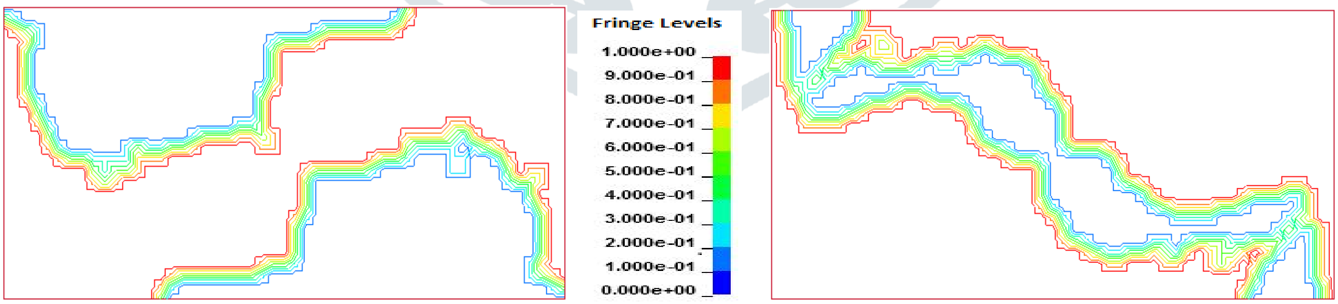

Top Layer at 2.1 ms **Bottom Layer at 2.1 ms**

Failure of Matrix in Tension mode

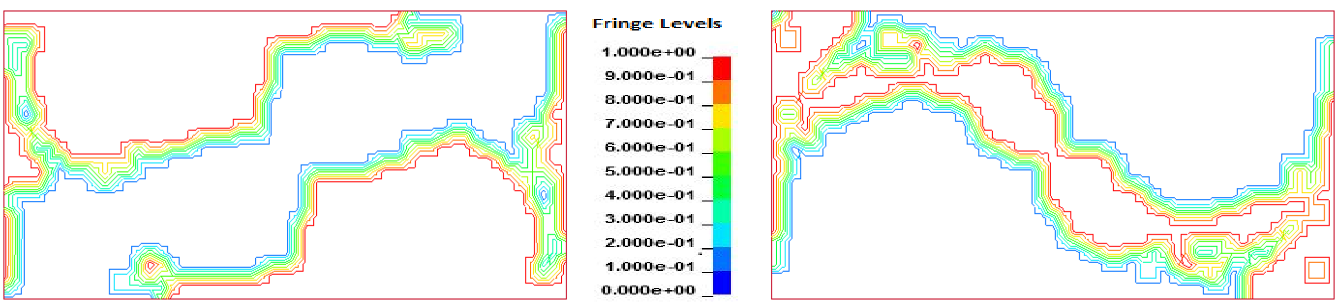

Top Layer at 2.1 ms **Bottom Layer at 2.1 ms**

Failure of Matrix in Compression mode

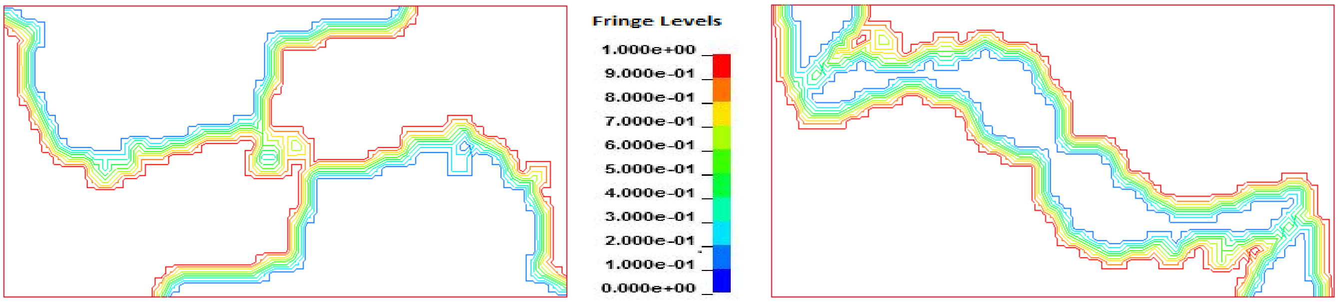

Top Layer at 2.1 ms **Bottom Layer at 2.1 ms**

Figure 17 Fibre and matrix failure contours

V. SINGLE SHELL WITH STIFFENER

The stiffened panel consists of the laminated composite plate provided with stiffeners in the longitudinal and/or transverse direction. As discussed above the stiffened panels are used widely in the automotive and aerospace sectors because of their energy absorption capability. The effect of the stiffener on the impact response of the composite laminate is studied. Figure 18 shows the geometric model of the single shell laminate with the stiffener.

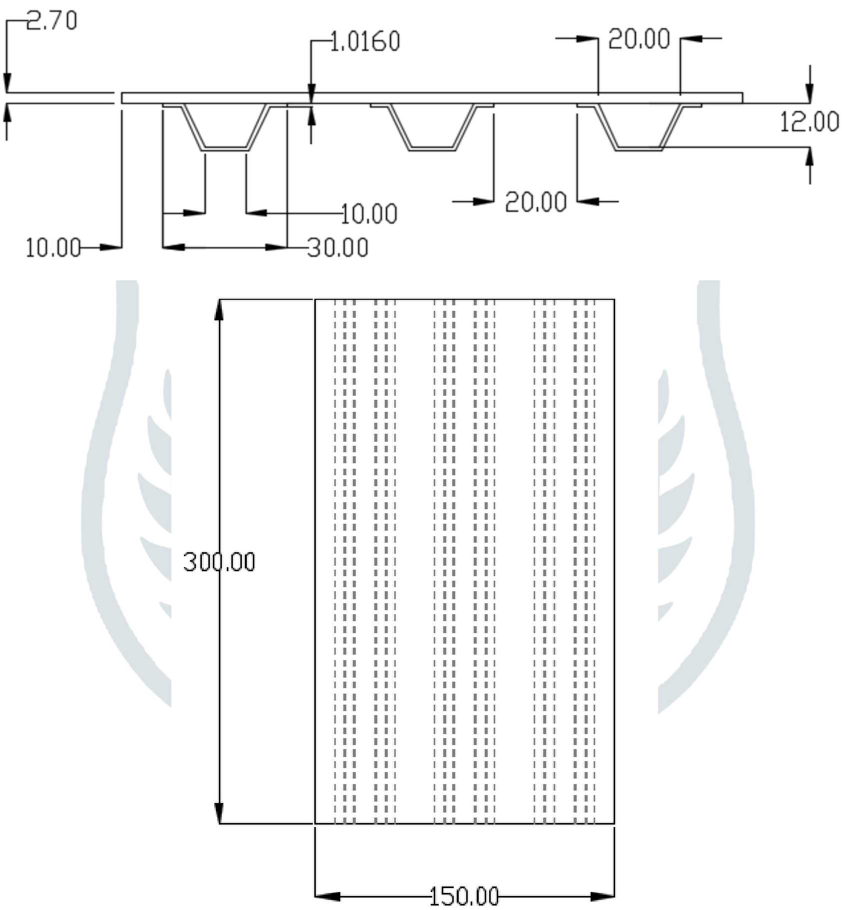

Figure 18 CAD geometry of the Single shell laminate with stiffener (All dimensions are in mm)

The properties of the stiffener are taken from work carried out by L. Marin et al [11]. Table 2 shows the properties of the stiffener. The stiffener is having a thickness of 1.016 mm, it contains 8 plies having the orientation of [90°/45°/-45°/0]$_S$ [12].

Table 2 Material properties of the stiffener [11].

Parameters	ρ [g/cm³]	E_{11} [GPa]	E_{22} [GPa]	E_{12} [GPa]	υ_{12} [-]	XT [MPa]	XC [MPa]	YT [MPa]	YC [MPa]	SC [MPa]
Defined Value	1.59	134.7	7.7	5.2	0.369	2290.5	1051	41.43	210	69.4

5.1 Finite element modeling

The finite element modeling of the laminate and the stiffener is shown in Figure 19. The laminate and the stiffener are modeled using Belytschko-Lin-Tsay shell element and the impactor was modeled using solid element. The boundary conditions and the impactor velocity remains the same as in single shell modeling.

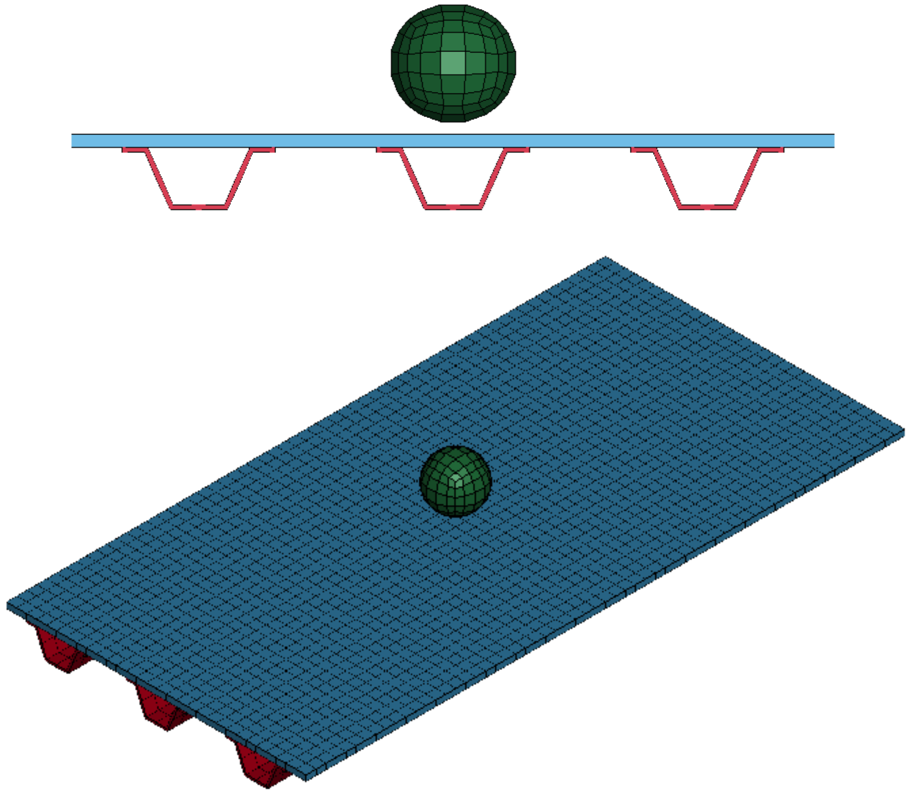

Figure 19 Finite Element Model of Single shell laminate with Hat stiffener

5.2 Results and Discussion

5.2.1 Energy plot

The Energy v/s Time history for a stiffened laminate is shown in Figure 20. From the figure, it is seen that there is an increase in the energy absorption by the laminate as compared to the benchmark problem, this is due to the presence of Stiffener. The maximum energy absorption was found to be 16.2 J.

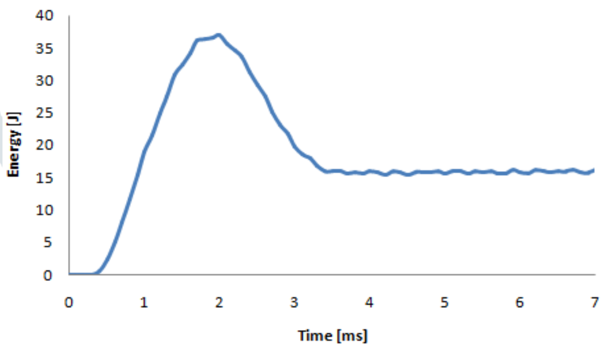

Figure 20 Energy plot for stiffened laminate

5.2.2 Impact contact force history

The stiffness of the composite laminate is high due to stiffener; hence the impact contact force response is increased. The maximum impact force was found to be 14.21 kN. The impact contact force history for a single shell with stiffener is shown in Figure 21.

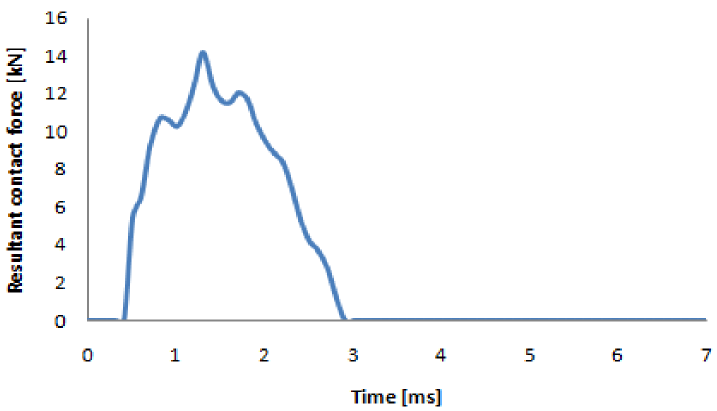

Figure 21 Impact contact force history

5.2.3 Displacement plots

The displacement of the stiffened laminate was 4.75 mm which is very small as compared to the composite laminate without stiffener. The displacement v/s time history is shown in Figure 22.

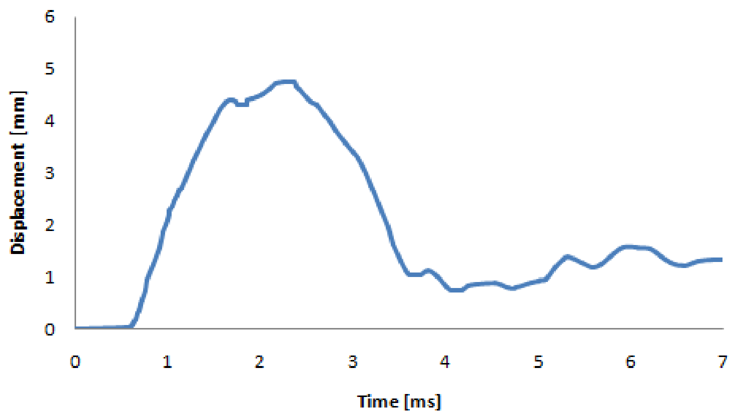

Figure 22 Displacement v/s time history

VI. INFLUENCE OF IMPACTOR SHAPE

This study deals with the effect of impactor shape on the low velocity impact response of a stiffened single shell composite laminate. The variation of the impact characteristics such as maximum contact force, energy absorbed and the intralaminar failures are studied and the results indicate that the projectile or impactor shape highly affects the impact response of the composite laminate.

The different types of impactors that are used are Spherical, Cylindrical and Conical Impactor. Figure 23 shows the geometry of all the three impactors. Here all the impactors are having a mass of 1.85 kg and the impact velocity is 6.5 m/s.

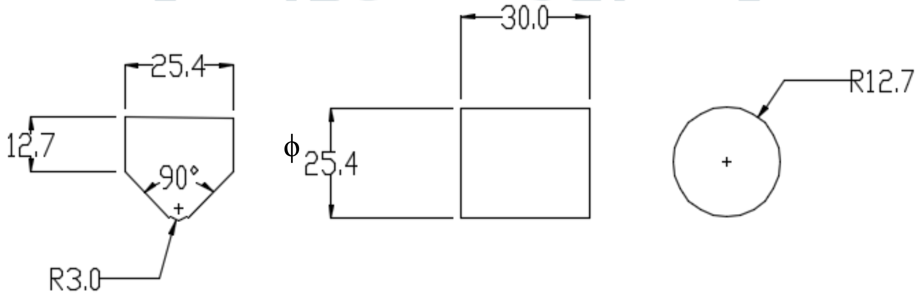

Figure 23 Geometry of the Conical, Cylindrical and Spherical Impactor [2] [13]

The Finite Element models having the cylindrical and spherical model are shown in Figure 24. Whereas the finite element model with spherical impactor is similar as shown in Figure 19.

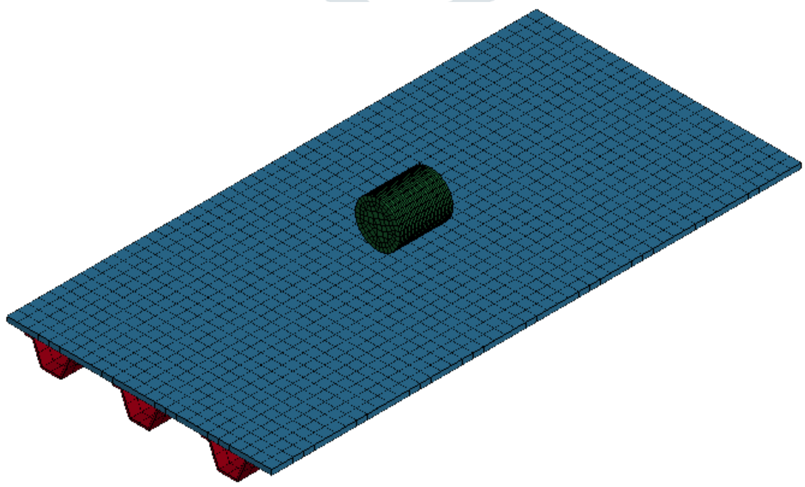

(a)

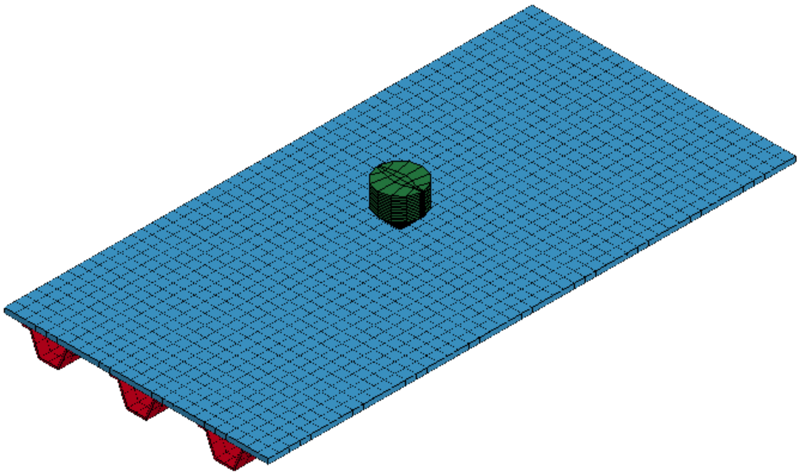

(b)

Figure 24 finite element models with (a) Cylindrical Impactor, (b) Conical Impactor

6.1 Results and Discussion

Figure 25 shows the Energy v/s Time history for all the three different impactors impacted on a stiffened composite laminate. Here all the impactors are impacted at on a laminate with the same velocity 6.5 m /s. From the Figure, it is seen that the energy absorption of the laminate impacted by comical impactor is larger as compared to laminates impacted by spherical and cylindrical impactors. The energy absorbed by the laminate when impacted by spherical, cylindrical and comical impactor was 16.2 J, 15.6J and 18.5J respectively

.

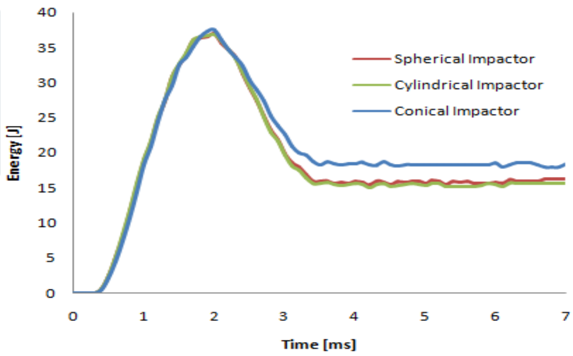

Figure 25 Influence of Impactor Shape on Energy plots

The resultant contact force v/s time history is shown in Figure 26. The resultant contact force is maximum in the laminate impacted by cylindrical impactor i.e. 15.3 kN, this is because the energy absorption is less compared to the other two types. The resultant contact force for spherical and cylindrical impactor is 14.2 kN and 11.7 kN respectively.

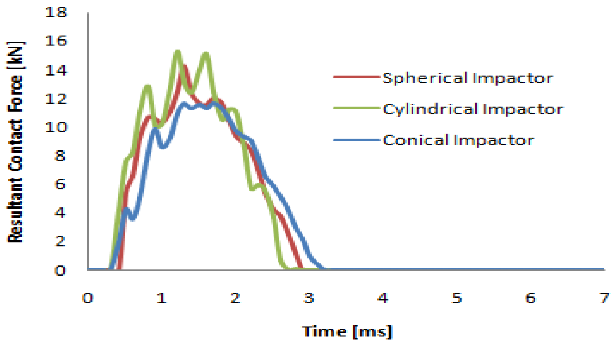

Figure 26 Influence of Impactor Shape on Contact force.

VII. CONCLUSION AND FUTURE STUDY

I this study, the low-velocity impact behaviour of the laminated carbon fibre/epoxy plate with and without stiffener was investigated using a commercial finite element tool LS-DYNA. The simulation results of the single shell laminate are compared with the experimental results. The simulation results showed a good correlation with a minimal percentage of error. Here along with the impact response such as impact energy plots, resultant contact force and displacement v/s time history, the intralaminar damages of the laminate have been studied.

Delamination study has been carried out by increasing the number of shell layers, two shell model has been created for this purpose with delamination contact interface between two shells. Tiebreak contact is used to develop the interface contact. From the results, it is seen that there is a reduction in stiffness due to delamination between the two shells. Intern which increases the energy absorption and reduces the resultant contact force but, there is an increase in the displacement of the shell. Therefore, an increase in delamination contacts or the number of shell layers will reduce the stiffness of the laminate. Results showed that material models used for modeling the laminate have a great influence on the impact response. Impact response of the stiffened panels has been carried out, results showed that adding the stiffener with the laminate will give that better results compared to the laminates without stiffener. Influence of the impactor shape on the impact response have been studied, the conical impactor has larger energy absorption as compared to the spherical and cylindrical impactors.

In the future study the influence of lot many parameters such as element size, no of shell layers, penalty stiffness, material models, impact positions, element type and delamination contact parameters such as NFLS, SFLS, and CCRIT.

VIII. Acknowledgement

The author sincerely expresses the gratitude to Mr Manjunath S. B. Assistant Professor, for his continuous guidance and support. The author thanks all the faculty of the Mechanical Engineering Department for their encouragement and invaluable advice.

References

[1] Abrate, S. 1998. Impact on Composite Structures, Cambridge University Press.
[2] Debabrata Chakraborty. 2007. Delamination of Laminated Fiber Reinforced Plastic Composites under Multiple Cylindrical Impact, Materials and Design 28, 1142–1153.
[3] K. Kaw. 2006. Mechanics of Composite Materials, Taylor and Francis Group, LLC.
[4] Robin Olsson. 2007. Experimental Validation of Delamination Criterion for Small Mass Impact, 16th International conference on composite materials, Japan.
[5] Hemendra Kumar Jain, Akhil Upadhyay. 2009. Laminated Composite Stiffened Panels: Applications And Behaviour. Civil Engineering Conference Innovation Without Limit (CEC-09), NIT Hamirpur, 89-96.
[6] Sebastian Heimbs, Sven Heller, Peter Middendorf. 2008. Simulation of Low-Velocity Impact on Composite Plates with Compressive Preload. LS-DYNA Anwenderforum, Bamberg.
[7] Sanan H Khan, Ankush P Sharma, Venkitanarayanan Parameswaran. 2017. An Impact induced damage in composite laminates with intra-layer and inter-laminate damage. Procedia Engineering 173, 409 – 416.
[8] Fatih Dogan, Homayoun Hadavinia, Todor Donchev, Prasannakumar S. Bhonge. 2012. Delamination of Impacted Composite Structures by Cohesive Zone Interface Elements and Tiebreak Contact. Materials Science and Engineering Faculty Research & Creative Works, Missouri, University of Science and Technology.
[9] G. A. Schoeppner, S. Abrate. 2000. Delamination Threshold Loads for Low Velocity Impact on Composite Laminate. Composite Part A: Applied Science and Manufacturing, Volume 31, 903-915
[10] Priyanjali Chatla. 2012. LS-DYNA for Crashworthiness of Composite Structures. University of Cincinnati.
[11] L. Marín, D. Trias, P. Badalló, G. Rus, J.A. Mayugo. 2012. Optimization of composite stiffened panels under mechanical and hygrothermal loads using neural networks and genetic algorithms. Composite Structures 94, 3321–3326 **.**
[12] Bo Cheng Jin. 2018. Design Optimization and Higher Order FEA of Hat-Stiffened Aerospace Composite Structures. Optimum Composite Structures. IntechOpen.
[13] Bulent Murat Icten, Binnur Goren Kiral. 2012. Impactor Shape Effect on Low Velocity Impact Response of Woven Glass Epoxy Composite. Advanced Composites Letter, Volume 21, Issue 5. 118-125